State of energy estimation for lithium-ion batteries using adaptive fuzzy control and forgetting factor recursive least squares combined with AEKF considering temperature.

LIU, D., WANG, S., FAN, Y., LIANG, Y., FERNANDEZ, C. and STROE, D.-I.

2023

State of Energy Estimation for Lithium-ion Batteries Using Adaptive Fuzzy Control and Forgetting Factor Recursive Least Squares Combined with AEKF Considering Temperature

Donglei Liu[1], Shunli Wang[12*], Yongcun Fan[1*], Yawen Liang[1], Carlos Fernandez[4], Daniel-Ioan Stroe[3]

[1]School of Information Engineering, Southwest University of Science and Technology, Mianyang 621010, China; [2]College of Electrical Engineering, Sichuan University, Chengdu 610065, China; [3]Department of Energy Technology, Aalborg University, Pontoppidanstraede 111 9220 Aalborg East, Denmark; [4]School of Pharmacy and Life Sciences, Robert Gordon University, Aberdeen AB10-7GJ, UK.

Abstract: As the main energy storage component of electric vehicles (EV), lithium-ion battery state estimation is an essential part of the battery management system (BMS). State of Energy (SOE) is one of the important state parameters, and its accurate estimation effectively reduces the potential safety hazards in the use of lithium-ion batteries, improves the efficiency of energy utilization, and alleviates the mileage anxiety of drivers. To solve the problem that the prediction of SOE of lithium-ion batteries is greatly influenced by temperature, a novel method called adaptive fuzzy control forgetting factor recursive least squares-Adaptive extended Kalman filtering (AFCFFRLS-AEKF) is formed. A fuzzy logic controller is designed for adaptive adjustment of the online parameter recognition forgetting factor with the change of working conditions. To solve the problem that the open-circuit voltage (OCV) changes with the influence of temperature in the variable temperature range, the regression analysis method is used in modeling to realize the regression analysis of OCV in a wide temperature range. Estimation accuracy is verified under two working conditions. The error of the estimation considering the temperature effect converges within 1%, which achieves higher estimation accuracy and stronger robustness.

*Corresponding author: Shun-Li Wang. Tel: +86-15884655563. E-mail address: 497420789@qq.com.

1   Introduction

1.1 Literature review

Battery SOE is defined as the percentage of battery remaining energy and rated capacity underrated working conditions[1, 2]. Compared with the state of charge (SOC), SOE not only describes the capacity characteristics of lithium-ion batteries but also reflects voltage changes [3]. Compared with SOC, SOE can reflect the real energy state of batteries more comprehensively and accurately [4]. Accurate estimation of battery SOE can enhance the reliability of estimation and prediction of power battery residual energy [5, 6]. There is a corresponding relationship between residual energy and battery range [7]. Accurate SOE estimation results can provide a reliable estimation basis for EV range prediction [8]. SOE as one of the important parameters of the vehicle BMS [9, 10], can be used as a vehicle energy optimization [11], reasonable distribution of battery power [12], to provide maximum energy to the motor [13], to extend the range of EV, improve the utilization efficiency of battery power [14], meet the dynamic performance of the vehicle, and is of great significance to improve the economic benefit of power battery [15]. It is of great significance to establish an equivalent circuit model to accurately characterize the electrochemical system of lithium-ion batteries for SOE estimation [16]. The lithium-ion battery is a complex electrochemical system, which is accompanied by a chemical reaction in the charging and discharging process, so the working mechanism of the lithium-ion battery is not a simple linear process, but a complex nonlinear electrochemical process[17]. The modeling of the lithium-ion electrochemical system needs to consider the complex electrochemical process, and various state parameters cannot be obtained directly [18]. Therefore, it is necessary to establish an appropriate battery model to describe the corresponding relationship between each chemical process and physical variables [19, 20]. So far, lithium-ion battery models can be divided into the electrochemical model [21], equivalent circuit model [22-24], artificial intelligence model using data[25-27], and hybrid model [28]. The model parameters of a lithium-ion battery are affected by temperature, discharge rate, discharge depth, and health status[29]. Among various factors, the temperature has the greatest influence on the electrochemical reaction in lithium-ion batteries[30], which shows that the capacity of lithium-ion batteries varies greatly at different temperatures. The OCV of lithium-ion batteries also varies at different temperatures. Even under extremely low temperatures, the lithium-ion battery cannot normally supply power due to too low temperature [31]. Therefore, it is necessary to consider the influence of temperature on lithium-ion batteries in equivalent modeling of the

working temperature range of lithium-ion batteries [32].

Lu et al. [33]studied the mechanism of heat generation of lithium-ion batteries and constructed a battery heat conduction model based on fractional calculus theory, which can well simulate the transient temperature field of batteries. Han et al. [34] established an improved semi-empirical capacity degradation model of lithium-ion battery that fully considered internal resistance and temperature, used a wavelet packet to de-noise the data set of the lithium-ion battery, and used a genetic algorithm to identify the parameters of the model, which can accurately predict the remaining service life and health status of lithium-ion battery. Moosavi et al. [35] based on the thermal analysis model of the temperature field of the cylindrical lithium-ion battery, etc., studied the important parameters of the temperature rise and thermal gradient of lithium-ion battery on the safety evaluation and performance of the lithium-ion battery. The research shows that the 21700 battery has the best thermal performance in high charge and discharge applications. Based on the pseudo-two-dimensional (P2D) model, Wang et al. [36] established a simplified discrete electrochemical model applicable to a wide temperature range by fitting lithium-ion concentration into a parabolic form. To reduce the influence of temperature on the SOC estimation accuracy of the lithium-ion battery, Wu et al. [37] took polymer ternary lithium-ion battery as the research object and established Thevenin equivalent circuit model with temperature compensation. UKF algorithm was used to estimate SOC, and the maximum error was within 3%. In this paper, a second-order RC equivalent circuit model is established to accurately characterize the characteristic parameters of lithium-ion batteries. Zhang et al. [38] analyzed the OCV characteristics of large-capacity batteries at different temperatures, and the results showed that the battery quality had a significant impact on voltage characteristics. Sheng et al [39] et al. characterized the specific heat and heat production rate of electrochemical cells by introducing a uniform temperature process to minimize the temperature difference between the cells. This new method can obtain the thermal performance of lithium-ion cells at a lower cost and in a shorter time. Shu et al.[40] proposed an adaptive fusion algorithm to robustly estimate the state of charge of lithium-ion batteries, using an improved recursive least square algorithm with a forgetting factor to identify the parameters of the proposed equivalent circuit model, verifying its effectiveness and stability in the presence of internal capacity degradation and operating temperature variation of the battery.

The temperature has a great influence on the performance of the lithium-ion battery and must be considered in the process of state estimation [41-43]. From the above literature analysis, it can be seen that the estimation method considering temperature modeling and filtering can effectively solve the influence of temperature in the process of state estimation [44].

The analytical modeling and online identification of lithium-ion batteries directly affect the state estimation of lithium-ion batteries [45, 46]. The establishment of a lithium-ion battery model considering temperature and discharge rate can effectively improve the accuracy of state estimation to a large extent [47].

In this paper, on the premise of fully analyzing the relationship between temperature and SOE in a wide temperature range of lithium-ion batteries, the model auto-regression online parameter identification considering the temperature is realized, and a good estimation effect is achieved. Temperature is an important factor to be considered in the modeling of lithium-ion batteries. The establishment of a lithium-ion battery model considering the influence of temperature can more accurately characterize the physical and chemical characteristics of the lithium-ion battery, and thus achieve the purpose of high-precision estimation of battery status. This study addresses the problem of temperature influence on the estimation of the SOE of lithium-ion batteries and completes the equivalent modeling and model-based parameter identification of the lithium-ion battery system using a combination of equivalent modeling considering temperature and fuzzy control adaptive online parameter identification to achieve an online estimation of the SOE of lithium-ion batteries.

1.2 Idea and contribution

Considering the temperature effect of OCV of the lithium-ion battery and the influence of model identification accuracy on energy state estimation, this paper adopts the idea of multilevel temperature curve regression analysis and fuzzy adaptive strategy based on forgetting factor recursive least square algorithm to solve the modeling and identification of lithium-ion battery model in a wide temperature range. Based on the model parameters and adaptive extended Kalman filtering algorithm, the SOE of lithium-ion batteries in a wide temperature range can be estimated with high accuracy and strong robustness. The main contributions of this paper are as follows.

(1) Based on the improved dual-polarization model, the coupling relationship among OCV, SOE, and temperature is established, and the OCV of the model can be accurately obtained in the wide temperature range of -5℃ to 35℃.

(2) A fuzzy adaptive online parameter identification strategy is designed, and the real-time online acquisition of all parameters of the improved dual-polarization model in the wide temperature range of -5℃ to 35℃ is realized according to the operating condition information.

(3) The adaptive extended Kalman filtering algorithm considering the temperature is constructed, and the adaptive correction of filtering noise in the wide temperature range of -5℃ to 35℃ is realized.

(4) A new adaptive fuzzy control forgetting factor recursive least squares-adaptive extended Kalman filtering method (AFCFFRLS-AEKF) is proposed, and the high accuracy and strong robustness of SOE estimation are verified by experiments.

1.3 Paper organization

The rest of this paper is organized as follows: In the second section, the improved dual-polarization equivalent circuit model is established, the fuzzy adaptive online identification strategy is designed, the adaptive extended Kalman filtering algorithm considering the temperature is constructed, and the adaptive fuzzy control-forgetting factor recursive least squares-adaptive extended Kalman filtering method (AFCFFRLS-AEKF) for estimating the energy state of lithium batteries is presented. In the third section, based on the experimental data, the multi-level temperature regression surface in a wide temperature range is obtained, and the estimation accuracy and robustness of the algorithm are discussed under two dynamic stress test conditions. The fourth section gives the conclusion.

2 Mathematical analysis

2.1 Equivalent circuit model

The lithium-ion battery is a complex electrochemical system. Due to the conversion of chemical energy, electric energy, and heat energy in the charging and discharging process, the lithium-ion battery has a strong nonlinear nature. To facilitate the analysis and calculation of state parameters of the lithium-ion battery, such as state of charge, SOE, state of power, state of health, and state of equilibrium, it is very important to build the equivalent circuit model of the battery. At present, the modeling of the lithium-ion battery can be divided into the electrochemical model, equivalent circuit model, artificial intelligence model using data, and hybrid model. The electrochemical model needs to analyze the complex internal reaction mechanism and is difficult to be applied in engineering practice due to a large amount of calculation. It is mainly used in the process of battery design and manufacturing. The artificial intelligence model can theoretically complete the equivalent modeling of the battery, but the training of the model requires a large number of actual operation data of the evaluated object, which cannot be modeled quickly and takes a long time to process, limiting its application. The equivalent circuit model with low complexity and clear physical and chemical significance has been widely used. The hybrid model selects a variety of models for equivalent modeling, which improves the modeling accuracy and increases the difficulty of modeling. In this paper, the equivalent circuit model is used to characterize the nonlinear electrochemical system of lithium-ion batteries. To

accurately characterize the dynamic characteristics of the electrochemical system of lithium-ion batteries, a dual-polarization model based on the Thevenin equivalent circuit model is used. The dual-polarization circuit model of the lithium-ion battery is shown in Fig. 1.
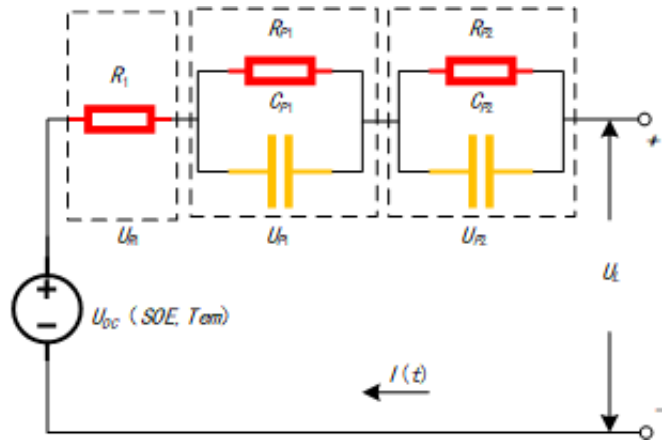
Fig. 1 The dual-polarization circuit model of lithium-ion battery

In Fig. 1, R_1 represents the polarization caused by the ohmic internal resistance of the lithium-ion battery, called ohmic polarization, and the voltage at both ends is U_{R1}. The voltage across the DC power supply is $U_{OC}(SOE, Tem)$, which is used to characterize the OCV of lithium-ion batteries changing with temperature and SOE. The polarization phenomenon caused by the electrochemical reaction velocity on the positive and negative electrodes being less than the electron movement velocity is regarded as electrochemical polarization, which is represented by the parallel connection of a resistor R_{P1} and a capacitor C_{P1}, and the voltage at both ends is U_{P1}. The polarization phenomenon caused by the diffusion rate of lithium-ions in the solid phase is less than the electrochemical reaction rate, which is regarded as the concentration difference polarization and characterized by the parallel connection of a resistor R_{P2} and a capacitor C_{P2}, and the voltage at both ends is U_{P2}. The subdivided battery model is called the second-order RC model because it consists of two RC loops in series. The second-order RC model of the lithium-ion battery can better characterize the dynamic properties of the battery without increasing the amount of calculation.

According to the established equivalent circuit model, Kirchhoff's law can be used to obtain the calculation formula of discharge voltage U_L and discharge current I(t) of the lithium-ion battery, as shown in Equation (1). The discharge voltage of the lithium-ion battery is the OCV minus the polarization voltage of each part. Because the two parts of electrochemical polarization and concentration difference polarization are connected in series, the current flowing through the two parts is

equal.

$$\begin{cases} U_L = U_{OC}(SOE, Tem) - U_{R1} - U_{P1} - U_{P2} \\ I(t) = C_{P1}\dfrac{dU_{P1}}{dt} + \dfrac{U_{p1}}{R_{p1}} = C_{P2}\dfrac{dU_{P2}}{dt} + \dfrac{U_{p2}}{R_{p2}} \end{cases} \tag{1}$$

The formula for SOE is shown in Equation (2). Taking parameters SOE, $U_{P1,}$ and U_{P2} as state variables, the state space equation of lithium-ion battery can be obtained according to Equation (1)and the zero-state response characteristic of the capacitor, as shown in Equation(3) **Error! Reference source not found.**and Equation (4)**Error! Reference source not found.**. Where the current $I(t)$ is discharged as positive and charged as negative.

$$SOE(k+1) = SOE(k) - I(k)\frac{\eta U_L(k-1)\Delta t}{E_N} \tag{2}$$

$$\begin{bmatrix} SOE(k+1) \\ U_{P1}(k+1) \\ U_{P2}(k+1) \end{bmatrix} = \begin{bmatrix} 1 & 0 & 0 \\ 0 & e^{-\frac{\Delta t}{R_{P1}C_{P1}}} & 0 \\ 0 & 0 & e^{-\frac{\Delta t}{R_{P2}C_{P2}}} \end{bmatrix} \times \begin{bmatrix} SOE(k) \\ U_{P1} \\ U_{P2} \end{bmatrix} + \begin{bmatrix} -\frac{\eta U_L(k-1)\Delta t}{E_N} \\ R_{P1}\left(1 - e^{-\frac{\Delta t}{R_{P1}C_{P1}}}\right) \\ R_{P2}\left(1 - e^{-\frac{\Delta t}{R_{P2}C_{P2}}}\right) \end{bmatrix}[I(t)] + \begin{bmatrix} \omega_{1,k} \\ \omega_{2,k} \\ \omega_{3,k} \end{bmatrix} \tag{3}$$

$$U_{L,k} = U_{oc,k}(SOE, Tem) - R_{1,k}I_k + \begin{bmatrix} 0 \\ -1 \\ -1 \end{bmatrix}^T \begin{bmatrix} SOE_k \\ U_{P1,k} \\ U_{P2,k} \end{bmatrix} + v_k \tag{4}$$

In Equation (3)**Error! Reference source not found.**, Δt represents the sampling interval, ω is the process noise in modeling and calculation, and the process noise is the zero-mean white noise whose covariance matrix is Q. v refers to the noise existing in the sensor or data reading. The measurement noise is zero-mean white noise with the covariance matrix R.

2.2 Adaptive fuzzy parameter identification and temperature surface

The OCV (U_{OC}) of lithium-ion batteries is affected by many factors, such as temperature and energy state, charge state, health state, remaining life, and so on. When the lithium-ion battery is in a state of extremely low temperature, it is very likely to be unable to work properly due to the increase in internal resistance and the decrease in chemical activity. Temperature and energy state are two important factors affecting the electrochemical reaction in lithium-ion batteries. The external voltage characteristics of lithium-ion batteries are important parameters in the battery power supply process, and also the observation object used to correct the filtering algorithm deviation. Therefore, obtaining accurate OCV in the charging and discharging process is an important link for parameter identification and high-precision state estimation of

lithium-ion batteries. The OCV of a lithium-ion battery can be measured only after the battery is charged and discharged for

a long time and the polarization of the battery disappears, that is, the polarization voltage of each part disappears. According

to the experimental guide 《Freedom CAR Battery Test Manual For Power-Assist Hybrid Electric Vehicles》, the HPPC

experiment with SOE divided into 10 levels was selected. Considering the operating temperature range of lithium-ion battery,

the temperature can be divided into 6 levels: -5℃, 5℃, 10℃, 15℃, 25℃, and 35℃, which can cover the temperature range

from -5℃ to 35℃. Statistical regression analysis was used to fit the nonlinear surface of the OCV of the lithium-ion battery.

Laplace transform is used to transform the dual-polarization circuit model described by Equation (1), and the complex

frequency domain expression of the constructed model can be obtained, as shown in Equation (5).

$$U_{OC}(s) - U_L(s) = I(s) \frac{R_1 s^2 + \frac{1}{\tau_1 \tau_2}(R_0\tau_1 + R_0\tau_2 + R_{P1}\tau_2 + R_{P2}\tau_1)s + \frac{R_1 + R_{P1} + R_{P2}}{\tau_1 \tau_2}}{s^2 + \frac{(\tau_1 + \tau_2)s}{\tau_1 \tau_2} + \frac{1}{\tau_1 \tau_2}} \tag{5}$$

In the formula $\tau_1 = R_{P1}\,C_{P1}$, $\tau_2 = R_{P2}\,C_{P2}$. The mode identification of the effect circuit using bilinear transformation, let

$s = \frac{2}{T}\frac{1-z^{-1}}{1+z^{-1}}$, where T is the sampling time, discretization of Equation (5), and the transfer function of the equivalent model

of a lithium-ion battery can be obtained as shown in Equation(6).

$$G(Z^{-1}) = \frac{c_3 + c_4 Z^{-1} + c_5 Z^{-2}}{1 - c_1 Z^{-1} - c_2 Z^{-2}} \tag{6}$$

In Equation(6), c_1, c_2, c_3, c_4, and c_5 are constants that need to be identified for parameter identification, and the equation

of lithium-ion battery is transformed into a linear difference equation, as shown in Equation (6).

$$y(k+1) = U_{OC} - U_L = c_1 y(k-1) + c_2 y(k-2) + c_3 I(k) + c_4 I(k-1) + c_5 I(k-2) \tag{7}$$

$I(k)$ is the system input and $y(k)$ is the system output in Equation (7). The relationship between lithium-ion battery

parameters and constant-coefficient can be derived, as shown in Equation (8).

$$\begin{cases} R_1 = \dfrac{c_3 - c_4 + c_5}{1 + c_1 - c_2} \\[2mm] \tau_1 \tau_2 = \dfrac{T^2(1 + c_1 - c_2)}{4(1 - c_1 - c_2)} \\[2mm] \tau_1 + \tau_2 = \dfrac{T(1 + c_2)}{1 - c_1 - c_2} \\[2mm] R_1 + R_{P1} + R_{P2} = \dfrac{c_3 + c_4 + c_5}{1 - c_1 - c_2} \\[2mm] R_1\tau_1 + R_1\tau_2 + R_{P1}\tau_2 + R_{P2}\tau_1 = \dfrac{T(c_3 - c_5)}{1 - c_1 - c_2} \end{cases} \tag{8}$$

The process of parameter identification is to use the charging and discharging data of the real-time operation of a lithium-ion battery to identify the parameter variables and reverse solve the equivalent parameters. The expression of input variables and parameter variables in the form of the matrix can obtain the formula as shown in Equation (9).

$$\begin{cases} \phi(k) = [y(k-1)\ y(k-2)\ I(k)\ I(k-1)\ I(k-2)] \\ \theta = [a_1\ a_2\ a_3\ a_4\ a_5] \end{cases} \tag{9}$$

Thus, the output matrix expression of the system can be obtained, as shown in Equation (10).

$$y(k) = \phi(k)^T \theta + e(k) \tag{10}$$

The forgetting factor recursive least square algorithm is used to identify the parameters of the equivalent circuit identification model online. The online parameter identification method can better adjust the parameters of the equivalent circuit model according to the dynamic characteristics and real-time operation data of lithium-ion batteries, to achieve the purpose of high-precision battery state estimation. The formula of the recursive least squares forgetting factor algorithm is shown in Equation (11).

$$\begin{cases} K(k+1) = P(k)\phi(k+1)[\rho + \phi^T(k+1)P(k)\phi(k+1)]^{-1} \\ \hat{\theta}(k+1) = \hat{\theta}(k) + K(k+1)\left[y(k+1) - \phi^T(k+1)\hat{\theta}(k)\right] \\ P(k+1) = \frac{1}{\rho}[I - K(k+1)\phi^T(k+1)]P(k) \end{cases} \tag{11}$$

In the formula, the forgetting factor ρ is the forgetting factor, $\hat{\theta}(k)$ is the solution of the desired quantity at time k, $\varphi(k)$ is the input matrix at time k, $K(k+1)$ is the gain at time $k+1$, and $P(k)$ is the covariance at time k. The traditional forgetting factor recursive least-squares algorithm generally takes a constant value between 0.95 and 1 to eliminate the phenomenon of "data saturation" caused by the increase of the data volume and the gradual approach to zero of the gain matrix.

The value of the forgetting factor directly affects the result of parameter identification. The forgetting factor with constant value cannot adapt to the dynamic electrochemical reaction in a lithium-ion battery with the update of real-time data. According to the real-time estimation error of the ion battery, the value of the forgetting factor can be adjusted adaptively to better analyze the electrochemical reaction trend mapped behind the data. A fuzzy logic controller was used to adjust the forgetting factor according to the identification error of the lithium-ion battery. The residuals and their mean values of the identified charge-discharge voltages were taken as the input of the fuzzy logic controller, and the adjustment value of the forgetting factor was taken as the output. A fuzzy logic controller with double input and single output was

designed for adaptive tuning calculation of the adjustment value of the forgetting factor. Seven fuzzy languages {NB, NM, NS, M, PS, PM, PB} are selected to describe the residual and mean values of charge and discharge voltages during the generation of fuzzy rules. The fuzzy sets are NB (negative big), NM (negative middle), NS (negative small), Z (zero), PS (positive small), PM (positive middle), and PB (positive big). Four fuzzy language variables {NB, NS, PS, PB} were selected to describe the adjustment value of the forgetting factor. The image of the input and output membership function of the fuzzy logic controller is shown in Fig. 2.
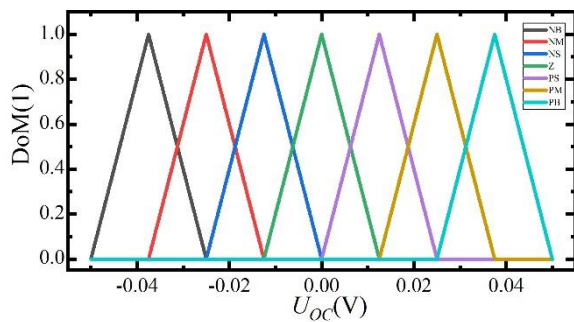
(a) Terminal voltage residual membership function
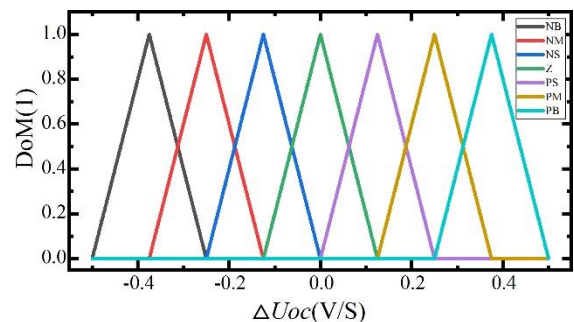
(b) Terminal-voltage residual mean membership function
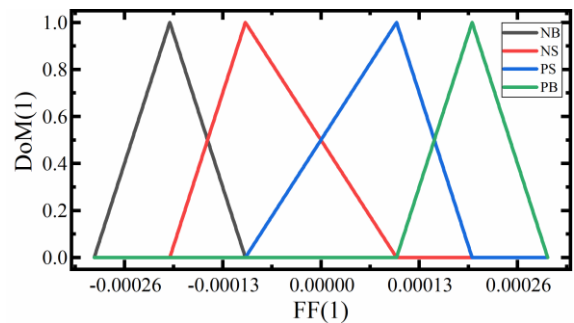
(c) Forgetting factor value membership function
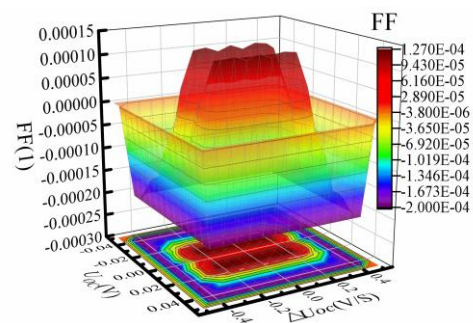
(d) Fuzzy regular surface diagram

Fig. 2 Fuzzy rule diagram

The value of the forgetting factor reflects the forgetting degree of the recursive least squares algorithm to the historical data. When the forgetting factor decreases, the influence of the old data on the system identification will be reduced, and the influence of the new data on the identification results will be double-enhanced. The output state NB indicates that the setting value of the forgetting factor decreases, while PB indicates that the setting value of the forgetting factor increases. The theoretical domain of charge and discharge voltage residuals is [-0.05, 0.05], the theoretical domain of mean charge and discharge voltage residuals are [-0.5, 0.5], and the theoretical domain of forgetting factor adjustment value is [-0.0003, 0.0003]. The membership function of each variable is adjusted and determined according to theoretical analysis and

simulation results, and a triangular membership function is used for all variables.

2.3 Adaptive extended Kalman filtering algorithm

When using the EKF algorithm to estimate battery SOE, its noise characteristics are assumed to be Gaussian white noise, but its characteristics can not be counted in practice. If white Gaussian noise is still assumed, the actual estimated error value of the system state will differ greatly from the theoretically calculated error value. With the continuous iteration of data, the estimated error will become larger and larger. This will reduce the estimation accuracy of the Kalman filtering algorithm and even invalidate it. To solve this problem, the AEKF algorithm, based on the EKF algorithm, continuously estimates and corrects the statistical characteristics of noise through the measurement data to improve the accuracy of system state estimation and realize the update of q_k, r_k, Q_k, R_k four noise variables. The updating process is shown in Equation (12).

$$\begin{cases} q_{k+1} = \dfrac{1}{k+1} G \sum_{i=0}^{k} \left(\hat{x}_{k+1} - A\hat{x}_k - Bu_k \right) \\[2mm] Q_{k+1} = \dfrac{1}{k+1} G \sum_{i=0}^{k} \left(K_{k+1}\tilde{y}_{k+1}\tilde{y}_{k+1}^T K_{k+1}^T + \tilde{P}_{k+1|k} - A\tilde{P}_{k+1|k}A^T \right) \\[2mm] r_{k+1} = \dfrac{1}{k+1} \sum_{i=0}^{k} \left(y_{k+1} - C\hat{x}_{k+1} \right) \\[2mm] R_{k+1} = \dfrac{1}{k+1} \sum_{i=0}^{k} \left(\tilde{y}_{k+1}\tilde{y}_{k+1}^T - C\tilde{P}_{k+1|k}C^T \right) \end{cases} \tag{12}$$

Where, $\hat{x}_k$ is the state of the system at the moment k; y_{k+1} is the observed quantity of state; G is noise-driven; A is the state transition matrix of the battery system; B is the control matrix; u_k is the control variable of the control matrix; C is the system measurement matrix; $\tilde{P}_{k+1|k}$ is the error covariance matrix of the initial prediction. In formula (11), the state observation y_{k+1} is a coupling function of temperature and SOE. Noise variables can be adaptively revised according to the changes in temperature and SOE.

$$y_k = f\left(Tem, SOE\right) \tag{13}$$

In the time-varying system of the lithium-ion battery, to better adapt to the changes in working conditions and internal chemical reactions of the lithium-ion battery, the A-weighting method is adopted to improve the estimator. The weighting coefficient $d_k = (1-b)/(1-b^{k+1})$ is used, where B is the forgetting degree of historical noise. The smaller the value of B is, the greater the weight of current data in the noise update. The calculation formula of the noise matrix after adding the weight coefficient is shown in Equation (14). According to the adaptive noise updating formula combined with the EKF recursive process, the AEKF algorithm process can be obtained, as shown in Equation (15).

$$
\begin{cases}
q_{k+1} = (1 - d_k)q_k + d_k G\left(\hat{x}_{k+1} - A\hat{x}_k - Bu_k\right) \\
Q_{k+1} = (1 - d_k)Q_k + d_k G\left(K_{k+1}\tilde{y}_{k+1}\tilde{y}_{k+1}^T K_{k+1}^T + \tilde{P}_{k+1|k} - A\tilde{P}_{k+1|k}A^T\right)G^T \\
r_{k+1} = (1 - d_k)r_k + d_k\left(y_{k+1} - C\hat{x}_{k+1} - Du_{k+1}\right) \\
R_{k+1} = (1 - d_k)R_k + d_k\left(\tilde{y}_{k+1}\tilde{y}_{k+1}^T - C\tilde{P}_{k+1|k}C^T\right)
\end{cases}
\tag{14}
$$

$$
\begin{cases}
\hat{x}_{k+1|k} = A\hat{x}_k + Bu_k + q_k \\
\tilde{P}_{k+1|k} = AP_k A^T + Q_k \\
K_k = \tilde{P}_{k+1|k}C^T\left(C\tilde{P}_{k+1|k}C^T + R_k\right)^{-1} \\
\tilde{y}_{k+1} = y_{k+1} - \left(C\hat{x}_{k+1|k} + Du_k\right) - r_k \\
\hat{x}_{k+1} = \hat{x}_{k+1|k} + K_k\tilde{y}_{k+1} \\
P_{k+1} = (E - K_k C)\tilde{P}_{k+1|k}
\end{cases}
\tag{15}
$$

In Equation (15), K_k is Kalman gain; R_k is measure noise; D is the driving prediction matrix; E is the identity matrix. After the calculation of Equation (15), the noise is updated by Equation (14) to realize the adaptive recursive iterative process of AEKF algorithm noise.

2.4 AFCFFRLS-AEKF algorithm

Based on equivalent modeling and adaptive parameter identification considering temperature, combined with the AEKF algorithm considering temperature, a novel SOE estimation method suitable for lithium-ion batteries in a wide temperature range is formed, which solves the problem of model identification and SOE estimation of lithium-ion battery in a wide temperature range. The resulting flow chart of the AFCFFRLS-AEKF algorithm is shown in Fig. 3.
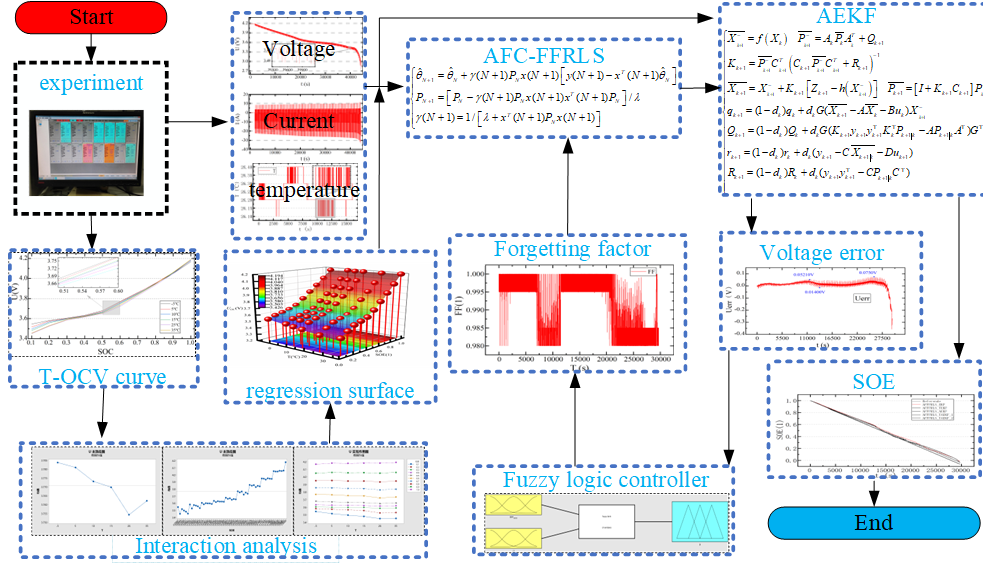
Fig. 3 AFCFFRLS-AEKF algorithm flow chart

In Fig. 3, charge and discharge data and temperature information of lithium-ion battery were obtained through experiments, and the OCV surface within a wide temperature range of lithium-ion battery was obtained through experimental analysis combined with regression analysis. Based on the voltage, current, and temperature information obtained in the experiment, the online parameter identification and SOE estimation of the equivalent model are realized. The voltage residual information was obtained during each estimation process, the AEKF noise information was updated according to the residual information, and a fuzzy logic controller was designed to adjust the forgetting factor of online parameter identification adaptively. The parameter identification results can better provide model parameter data for AEKF to estimate SOE, and to realize the online SOE estimation of lithium-ion batteries based on the AFCFFRLS-AEKF algorithm considering the influence of wide temperature.

3   Experiments and discussions

The experimental platform was built according to the experimental design, and the experimental instruments included a large rate charge and discharge tester (BTS-750-200-100-4), a three-layer independent thermostat, an industrial control computer, and a lithium-ion battery. According to the experiment design, experiments under different temperatures and SOE conditions were carried out and data were recorded. The basic technical parameters of the battery used are shown in Table.1.

Table. 1 Basic technical parameters of the battery

Factor	parameter
Size: length * width * height /mm	200*80*180

Rated voltage/V	3.65
Maximum load current /A	1.5C
Charge cut-off voltage/V	4.2
Discharge cutoff voltage/V	2.75
Working temperature /℃	-10~40
Rated capacity/Ah	70.0

3.1 Experimental platform and experiment

The experimental platform was built according to the experimental requirements to meet the requirements of fixed SOE charging and discharging of lithium-ion batteries and temperature control in the experiment. The experimental platform built is shown in Fig. 4.
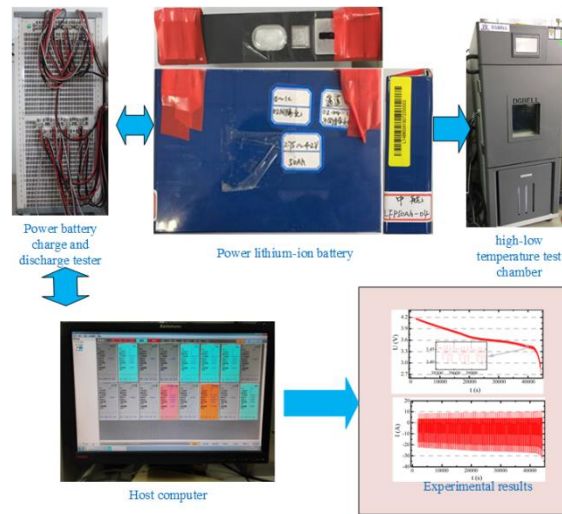
Fig. 4 Experimental platform diagram

The experiment design includes two factors: SOE and temperature, in which there are 10 levels of SOE and 6 levels of temperature. After input in Minitab software, a 60-time experimental schedule was made. According to the experiment plan, set the corresponding experiment steps on the industrial control computer, and adjust the thermostat to the corresponding temperature. The experimental results obtained based on the experimental data are shown in Table. 2.

Table. 2 OCV-SOE experimental results at different temperatures

Step	T℃	SOE	U_{OC}	Step	T℃	SOE	U_{OC}	Step	T℃	SOE	U_{OC}	Step	T℃	SOE	U_{OC}
1	-5	0.1	3.545	16	5	0.6	3.7658	31	15	0.1	3.4805	46	25	0.6	3.7224
2	-5	0.2	3.5813	17	5	0.7	3.8569	32	15	0.2	3.5571	47	25	0.7	3.8296
3	-5	0.3	3.6049	18	5	0.8	3.9533	33	15	0.3	3.5968	48	25	0.8	3.9347
4	-5	0.4	3.6328	19	5	0.9	4.0593	34	15	0.4	3.6228	49	25	0.9	4.0497

5	-5	0.5	3.6793	20	5	1	4.1827	35	15	0.5	3.6604	50	25	1	4.1818
6	-5	0.6	3.7686	21	10	0.1	3.496	36	15	0.6	3.7503	51	35	0.1	3.4539
7	-5	0.7	3.8594	22	10	0.2	3.5664	37	15	0.7	3.8457	52	35	0.2	3.5292
8	-5	0.8	3.9499	23	10	0.3	3.598	38	15	0.8	3.9462	53	35	0.3	3.5897
9	-5	0.9	4.0488	24	10	0.4	3.6241	39	15	0.9	4.0562	54	35	0.4	3.6204
10	-5	1	4.1672	25	10	0.5	3.6635	40	15	1	4.1827	55	35	0.5	3.656
11	5	0.1	3.5168	26	10	0.6	3.754	41	25	0.1	3.4508	56	35	0.6	3.736
12	5	0.2	3.5748	27	10	0.7	3.8485	42	25	0.2	3.5249	57	35	0.7	3.8395
13	5	0.3	3.6008	28	10	0.8	3.9468	43	25	0.3	3.5859	58	35	0.8	3.9453
14	5	0.4	3.6278	29	10	0.9	4.0547	44	25	0.4	3.6151	59	35	0.9	4.0606
15	5	0.5	3.6712	30	10	1	4.1793	45	25	0.5	3.6489	60	35	1	4.1914

Table. 2 records the results of 60 experiments. To verify the robustness of the algorithm, the dynamic stress test at 25℃ is used to verify whether the proposed algorithm has a strong robust estimation performance.

3.2 Temperature regression surface

The OCV surface of lithium-ion battery with temperature characteristics and its equation were obtained by experimental design combined with linear regression analysis. During the analysis, two temperature surfaces were obtained with or without the temperature of 25℃, which were used to verify the robustness of the fuzzy adaptive method to estimate the energy state of the powerful lithium-ion battery considering the influence of temperature. When considering the temperature condition of 25℃, the temperature surface obtained is shown in Fig. 5.
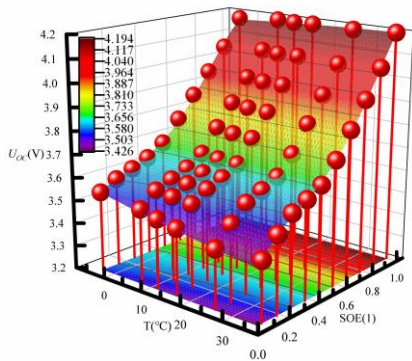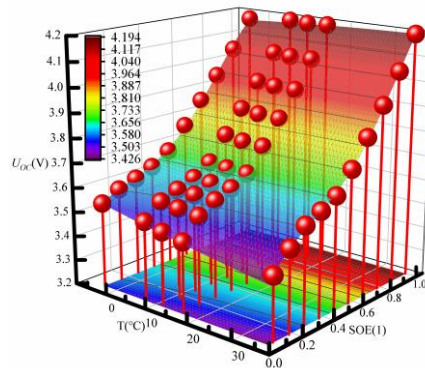
a. 6 horizontal temperature response surface   b. 5 horizontal temperature response surface

Fig. 5 Temperature regression surface

Fig. 5.a is a fitting surface with a temperature condition of 25℃. The regression analysis of this surface includes all 60 experimental data. The r-square value of the surface is 0.99817, and the adjusted r-square value is 0.99775, a difference of 0.00042, indicating that the surface has a good fit and effect at the temperature of 6. Fig. 5.b is a fitting surface excluding 25℃ temperature, in which case it can be used to verify the robustness of the nonlinear regression analysis equation for OCV prediction. The r-squared value of the surface is 0.99822, and the adjusted r-squared value is 0.99770, with a difference of 0.00052. The r-square value of surface fitting at the 5-level temperature is higher than that at the 6-level, but the fitting degree and effect are still very good. Put the 25℃ experimental data into the temperature surface of 5 temperature horizontal regression analysis, and the estimated error value can be obtained, as shown in Fig. 6.
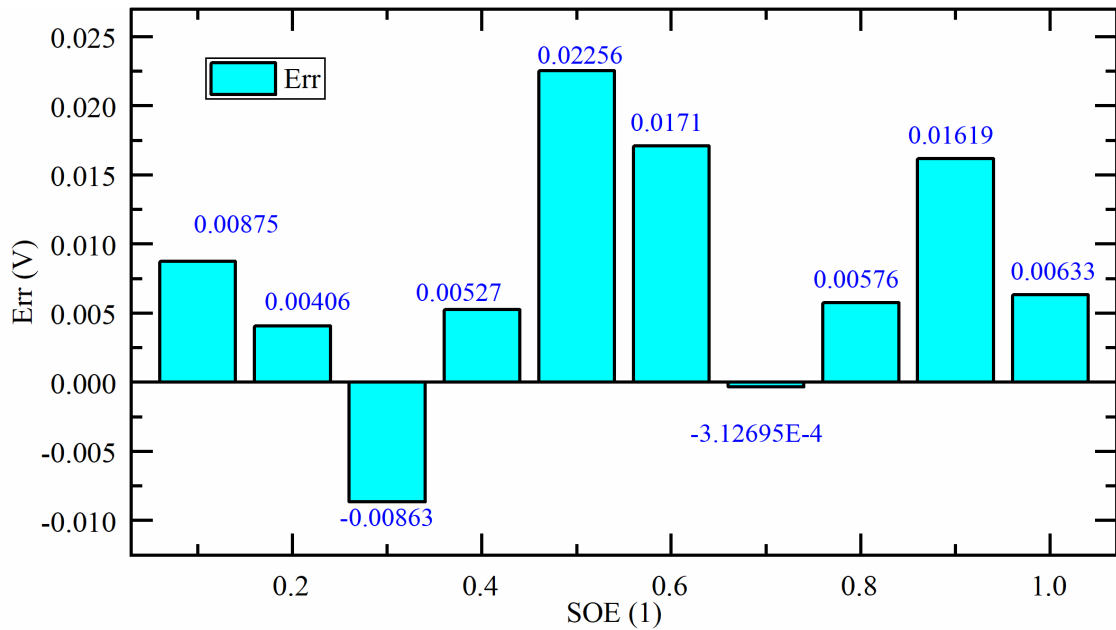
Fig. 6 Voltage estimation error diagram

Fig. 6 is the estimation error diagram of OCV at 25℃. After calculation, MAE, MAPE, and RMSE estimated are 0.950%, 0.254%, and 1.154% respectively. The results show that the experimental design combined with the regression analysis method can be used to estimate the OCV under unknown temperatures, which can effectively solve the problem of poor robustness of the model OCV under a wide temperature range.

3.3 DST experimental estimation results

The 6-level temperature response surface including 25℃ and the 5-level temperature response surface excluding 25℃ combined with a fuzzy adaptive control strategy were used to estimate the dynamic stress test (DST) experimental energy

state at 25℃. The estimated results are shown in Fig. 7.
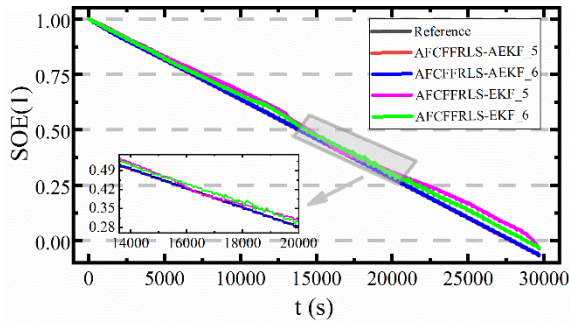
a. SOE estimation results
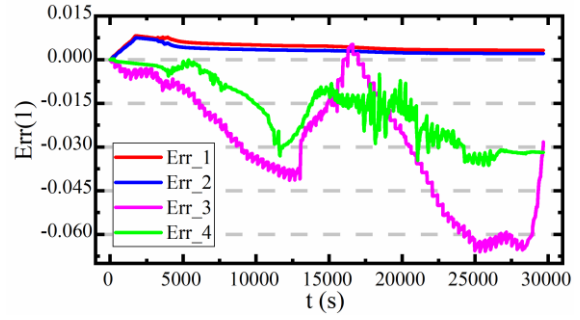
b. SOE estimation error

Fig. 7 The estimation result of SOE under 25℃ DST experimental condition

In Fig. 7, AFCFFRLS-AEKF_5 represents the result of SOE estimation using 5 horizontal temperature response surface and fuzzy control strategy combined with AEKF algorithm, Err_1 represents its estimation error, and the estimation error is within 1%. AFCFFRLS-AEKF_6 represents the result of SOE estimation using 6 horizontal temperature response surfaces and fuzzy control strategy combined with the AEKF algorithm. Err_2 represents its estimation error, and the estimation error is within 1%. AFCFFRLS-EKF_5 represents the result of SOE estimation using the 5-level temperature response surface and fuzzy control strategy combined with the EKF algorithm, Err_3 represents its estimation error, and the estimation error is within 7%. AFCFFRLS-EKF_6 represents the result of SOE estimation using the 6-level temperature response surface and fuzzy control strategy combined with the EKF algorithm, Err_4 represents its estimation error, and the estimation error is within 4%. MAE, MAPE, and RMSE results of the four algorithms are shown in Table. 3.

Table. 3 Error analysis table under 25℃ DST experimental condition

Method	AFCFFRLS-EKF_5	AFCFFRLS-EKF_6	AFCFFRLS-AEKF_5	AFCFFRLS-AEKF_6
MAE (%)	2.9016	1.7135	0.4515	0.3215
MAPE (%)	19.6352	10.4060	1.5206	0.1028
RMSE (%)	3.5569	2.0471	0.4724	0.3479

It can be seen in Table. 3 that the estimation accuracy of SOE using the adaptive Extended Kalman filtering algorithm is higher than that using the extended Kalman filtering algorithm, and the estimation accuracy of the 6-level temperature response surface is higher than that of the 5-level temperature response surface. From the perspective of MAE, the MAE of the AFCFFRLS-AEKF_6 algorithm is 0.3215, which proves that the predicted value of SOE can converge near the true

value in the whole prediction process. From the MAPE of SOE estimation error, the MAPE of the AFCFFRLS-AEKF_6 algorithm is 0.1028, which indicates that the constructed algorithm has good estimation accuracy. From the perspective of the quality of regression prediction, the RMSE of the AFCFFRLS-AEKF_6 algorithm is 0.3479, which has a good regression effect compared with the previous three cases.

3.4 BBDST experimental estimation results

The feasibility of the method was verified under Beijing Bus dynamic stress test (BBDST) working conditions. The experiment data was acquired at the temperature of 25℃. Similarly, the regression curve of two response surfaces is used to verify the estimation accuracy and robustness of the algorithm. The estimation accuracy of the algorithm can be verified when using a 6-level temperature response surface containing 25℃ OCV information. Furthermore, the robustness and accuracy of the algorithm can be verified when using a 5-level temperature response surface that does not contain 25℃ OCV information. The estimated results are shown in Fig. 8.

| a. SOE estimation results | b. SOE estimation error |
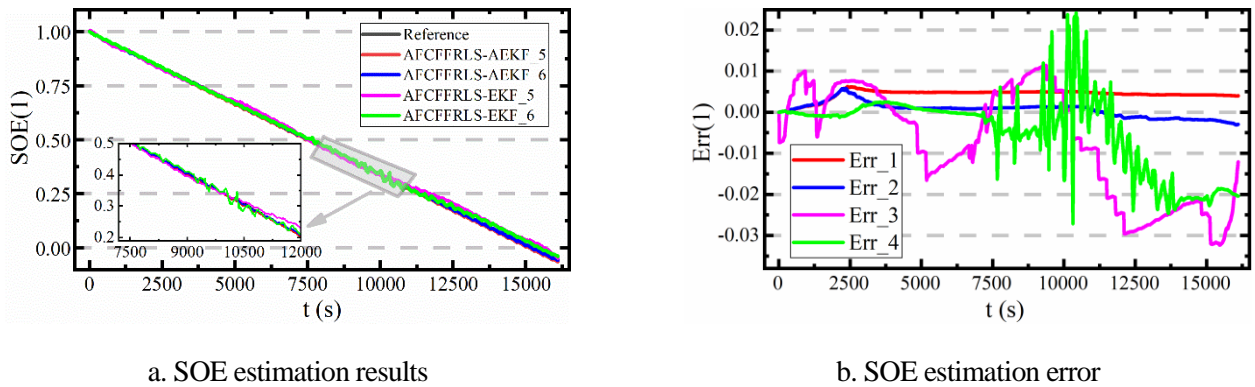
Fig. 8 The estimation result of SOE under 25℃ BBDST experimental condition

The naming rules in Fig. 8 are the same as in Fig. 7. The error 1 and error 2 can also converge to within 1% under the BBDST experimental conditions. Error 3 and error 4 converge to within 3.5%. Again for the convenience of analysis, the MAE, MAPE, and RMSE of the four algorithms were calculated and the results obtained are shown in Table. 4.

Table. 4 Error analysis table under 25℃ BBDST experimental condition

Method	AFCFFRLS-EKF_5	AFCFFRLS-EKF_6	AFCFFRLS-AEKF_5	AFCFFRLS-AEKF_6
MAE (%)	1.2312	0.6819	0.4357	0.1542
MAPE (%)	62.7449	42.6754	9.1058	3.7182

RMSE (%)	1.5383	1.0385	0.4515	0.1840

From the perspective of MAE, the MAE of the AFCFFRLS-AEKF_6 algorithm is 0.1542, which proves that the predicted value of SOE can converge near the truth value in the whole prediction process. From the MAPE of SOE estimation error, the MAPE of the AFCFFRLS-AEKF_6 algorithm is 3.7182, which indicates that the constructed algorithm has good estimation accuracy. From the perspective of the quality of regression prediction, the RMSE of the AFCFFRLS-AEKF_6 algorithm is 0.1840, which has a good regression effect compared with the previous three cases.

4   Conclusions

In view of the problem that the prediction of SOE of lithium-ion batteries is greatly affected by temperature, the equivalent model adaptive parameter identification considering the temperature is realized by using regression analysis and fuzzy logic control, and a novel (AFCFFELS-AEKF) SOE estimation method suitable for lithium-ion batteries in a wide temperature range is formed by combining AEKF algorithm considering the temperature. The regression analysis method is used to realize voltage estimation considering temperature, which is proved to have well estimation accuracy and regression effect. The applicability of the constructed estimation model is verified in two experimental conditions. The estimation errors of the estimation method considering the temperature effect can converge within 1% in both conditions, which can achieve high estimation accuracy and strong robustness.

References

1. Zhang, S.Z. and X.W. Zhang, *A novel low-complexity state-of-energy estimation method for series-connected lithium-ion battery pack based on "representative cell" selection and operating mode division.* Journal of Power Sources, 2022. **518**: p. 1-13.

2. Zhang, S.Z. and X.W. Zhang, *Joint estimation method for maximum available energy and state-of-energy of lithium-ion battery under various temperatures.* Journal of Power Sources, 2021. **506**: p. 1-18.

3. Zhang, S.Z. and X.W. Zhang, *A novel non-experiment-based reconstruction method for the relationship between open-circuit-voltage and state-of-charge/state-of-energy of lithium-ion battery.* Electrochimica Acta, 2022. **403**: p. 22-41.

4. Fan, T.E., et al., *Simultaneously estimating two battery states by combining a long short-term memory network with an adaptive unscented Kalman filter.* Journal of Energy Storage, 2022. **50**: p. 1163-1181.

5. Lu, L., et al., *A review on the key issues of the lithium-ion battery management.* Science & Technology Review, 2016.

34(6): p. 39-51.

6. Chen, Y.J., et al., *Remaining available energy prediction for lithium-ion batteries considering electrothermal effect and energy conversion efficiency.* Journal of Energy Storage, 2021. **40**: p. 117-138.

7. Li, X.Y., et al., *State of energy estimation for a series-connected lithium-ion battery pack based on an adaptive weighted strategy.* Energy, 2021. **214**: p. 64-85.

8. Xu, W., et al., *A Multi-Timescale Estimator for Lithium-Ion Battery state of Charge and State of Energy Estimation Using Dual H infinity Filter.* Ieee Access, 2019. **7**: p. 181229-181241.

9. Shrivastava, P., et al., *Combined State of Charge and State of Energy Estimation of Lithium-Ion Battery Using Dual Forgetting Factor-Based Adaptive Extended Kalman Filter for Electric Vehicle Applications.* Ieee Transactions on Vehicular Technology, 2021. **70**(2): p. 1200-1215.

10. Wang, Y.J., et al., *A comprehensive review of battery modeling and state estimation approaches for advanced battery management systems.* Renewable & Sustainable Energy Reviews, 2020. **131**: p. 125-148.

11. An, F.L., et al., *State of Energy Estimation for Lithium-Ion Battery Pack via Prediction in Electric Vehicle Applications.* Ieee Transactions on Vehicular Technology, 2022. **71**(1): p. 184-195.

12. Laadjal, K. and A.J.M. Cardoso, *A review of supercapacitors modeling, SoH, and SoE estimation methods: Issues and challenges.* International Journal of Energy Research, 2021. **45**(13): p. 18424-18440.

13. Guo, R.H. and W.X. Shen, *An enhanced multi-constraint state of power estimation algorithm for lithium-ion batteries in electric vehicles.* Journal of Energy Storage, 2022. **50**: p. 120-151.

14. Chang, J.Q., M.S. Chi, and T. Shen, *Model based state-of-energy estimation for LiFePO4 batteries using unscented particle filter.* Journal of Power Electronics, 2020. **20**(2): p. 624-633.

15. Sun, B., et al., *Study on the Economy of Energy Storage System with Lithium-Ion Battery Participating in AGC Auxiliary Service.* Transactions of China Electrotechnical Society, 2020. **35**(19): p. 4048-4061.

16. Shrivastava, P., et al., *Model-based state of X estimation of lithium-ion battery for electric vehicle applications.* International Journal of Energy Research, 2022. **46**(8): p. 10704-10723.

17. Shu, X., et al., *State of health prediction of lithium-ion batteries based on machine learning: Advances and perspectives.* Iscience, 2021. **24**(11): p. 1-25.

18. Ji, H., et al., *State of health prediction model based on internal resistance.* International Journal of Energy Research, 2020. **44**(8): p. 6502-6510.

19. Hu, X.S., et al., *State estimation for advanced battery management: Key challenges and future trends.* Renewable & Sustainable Energy Reviews, 2019. **114**: p. 22-48.

20. Long, B., et al., *Prognostics Comparison of Lithium-Ion Battery Based on the Shallow and Deep Neural Networks Model.* Energies, 2019. **12**(17): p. 56-73.

21. Ortiz-Ricardez, F.A., A. Romero-Becerril, and L. Alvarez-Icaza, *Residue grouping order reduction method in solid-phase lithium-ion battery models.* Journal of Applied Electrochemistry, 2021. **51**(12): p. 1635-1649.

22. Su, J., et al., *An equivalent circuit model analysis for the lithium-ion battery pack in pure electric vehicles.* Measurement & Control, 2019. **52**(3-4): p. 193-201.

23. Yu, D., et al., *Failure mechanism and predictive model of lithium-ion batteries under extremely high transient impact.* Journal of Energy Storage, 2021. **43**: p. 54-86.

24.   Xie, Y., et al., *A new method of unscented particle filter for high-fidelity lithium-ion battery SOC estimation.* Energy Storage Science and Technology, 2021. **10**(2): p. 722-731.

25.   Ma, L., C. Hu, and F. Cheng, *State of Charge and State of Energy Estimation for Lithium-Ion Batteries Based on a Long Short-Term Memory Neural Network.* Journal of Energy Storage, 2021. **37**: p. 25-52.

26.   Li, C., et al., *An Approach to Lithium-ion Battery Simulation Modeling Under Pulsed High Rate Condition Based on LSTM-RNN.* Proceedings of the Chinese Society of Electrical Engineering, 2020. **40**(9): p. 3031-3041.

27.   Liu, Y.F., et al., *State of Charge Estimation of Lithium-Ion Batteries Based on Temporal Convolutional Network and Transfer Learning.* Ieee Access, 2021. **9**: p. 34177-34187.

28.   Jiang, Y.Y., et al., *State of Health Estimation for Lithium-Ion Battery Using Empirical Degradation and Error Compensation Models.* Ieee Access, 2020. **8**: p. 123858-123868.

29.   Shu, X., et al., *Ensemble Learning and Voltage Reconstruction Based State of Health Estimation for Lithium-Ion Batteries With Twenty Random Samplings.* 2023: p. 1-11.

30.   Zhao, H., et al., *State of health estimation for lithium-ion batteries based on hybrid attention and deep learning.* Reliability Engineering and System Safety, 2023: p. 1-12.

31.   Barcellona, S. and L. Piegari, *Integrated electro-thermal model for pouch lithium ion batteries.* Mathematics And Computers In Simulation, 2021. **183**: p. 5-19.

32.   Feng, X.N., et al., *Investigating the thermal runaway mechanisms of lithium-ion batteries based on thermal analysis database.* Applied Energy, 2019. **246**: p. 53-64.

33.   Lu, X., H. Li, and N. Chen, *Analysis of the Properties of Fractional Heat Conduction in Porous Electrodes of Lithium-Ion Batteries.* Entropy, 2021. **23**(2): p. 88-115.

34.   Han, X., Z. Wang, and Z. Wei, *A novel approach for health management online-monitoring of lithium-ion batteries based on model-data fusion.* Applied Energy, 2021. **302**: p. 26-48.

35.   Moosavi, A., A.-L. Ljung, and T.S. Lundstrom, *Design considerations to prevent thermal hazards in cylindrical lithium-ion batteries: An analytical study.* Journal of Energy Storage, 2021. **38**: p. 25-52.

36.   Wang, D., et al., *A lithium-ion battery electrochemical-thermal model for a wide temperature range applications.* Electrochimica Acta, 2020. **362**: p. 23-48.

37.   Wu, X., X. Li, and J. Du, *State of Charge Estimation of Lithium-Ion Batteries Over Wide Temperature Range Using Unscented Kalman Filter.* Ieee Access, 2018. **6**: p. 41993-42003.

38.   Zhang, R., et al., *A Study on the Open Circuit Voltage and State of Charge Characterization of High Capacity Lithium-Ion Battery Under Different Temperature.* Energies, 2018. **11**(9): p. 56-67.

39.   Sheng, L., et al., *An improved calorimetric method for characterizations of the specific heat and the heat generation rate in a prismatic lithium ion battery cell.* Energy Conversion and Management, 2019. **180**: p. 724-732.

40.   Shu, X., et al., *An adaptive fusion estimation algorithm for state of charge of lithium-ion batteries considering wide operating temperature and degradation.* Journal of Power Sources, 2020. **462**: p. 1-31.

41.   Mei, W., et al., *Three-dimensional layered electrochemical-thermal model for a lithium-ion pouch cell.* International Journal of Energy Research, 2020. **44**(11): p. 8919-8935.

42.   Ji, H., et al., *State of health prediction model based on internal resistance.* International Journal of Energy Research, 2020. **44**(8): p. 6502-6510.

43.   Bayatinejad, M.A. and A. Mohammadi, *Investigating the effects of tabs geometry and current collectors thickness of lithium-ion battery with electrochemical-thermal simulation.* Journal of Energy Storage, 2021. **43**: p. 1104-1129.

44.   Lei, Z., Y. Zhang, and X. Lei, *Improving temperature uniformity of a lithium-ion battery by intermittent heating method in cold climate.* International Journal of Heat and Mass Transfer, 2018. **121**: p. 275-281.

45.   Pang, H., et al., *A novel extended Kalman filter-based battery internal and surface temperature estimation based on an improved electro-thermal model.* Journal of Energy Storage, 2021. **41**: p. 1204-1231.

46.   Andriunas, I., et al., *Impact of solid-electrolyte interphase layer thickness on lithium-ion battery cell surface temperature.* Journal of Power Sources, 2022. **525**: p. 874-896.

47.   Xu, X., et al., *Remaining Useful Life Prediction of Lithium-ion Batteries Based on Wiener Process Under Time-Varying Temperature Condition.* Reliability Engineering & System Safety, 2021. **214**: p. 263-285.